The trithorax protein partner menin acts in tandem with EZH2 to suppress C/EBPα and differentiation in MLL-AF9 leukemia

Austin T. Thiel, Zijie Feng, Dhruv K. Pant, Lewis A. Chodosh, and Xianxin Hua

Abramson Family Cancer Research Institute, Department of Cancer Biology, Abramson Cancer Center, the University of Pennsylvania, Perelman School of Medicine, Philadelphia, PA, USA

 doi:10.3324/haematol.2012.074195

Online Supplementary Design and Methods

Plasmids

The following plasmids were described elsewhere: pMIG-MLL-AF9-ires-GFP, pMSCVpgk-Hoxa9-GFP, pMSCVpac-Meis1A, and pcDNA3-CEBPA-HA.[1-3] Dr. Alan Friedman provided MigRI-CEBPA-ER. LZRS-Flag-EZH2-ER, pCMV-HA-EZH2 and lentiviral packaging plasmids, pMD2G and pAX2G were obtained from Addgene. Lentiviral shRNA targeting *EZH2* and pLKO.1 Scr control were purchased from Sigma, and shRNA targeting *MEN1* were purchased from Open Biosystems. The shRNA sequences are shown below.

Lentiviral shRNA

Sense-Loop-Antisense			
shMen1-1:	GCTGTACCTGAAAGGATCATA	CTCGAG	TATGATCCTTTCAGGTACAGC
shMen1-2:	GTGCAGATGAAGAAGCAGAAA	CTCGAG	TTTCTGCTTCTTCATCTGCAC
shEZH2-1:	GCTAGGTTAATTGGGACCAAA	CTCGAG	TTTGGTCCCAATTAACCTAGC
shEZH2-2:	CCCAACATAGATGGACCAAAT	CTCGAG	ATTTGGTCCATCTATGTTGGG
shEZH2-3:	TATGATGGTTAACGGTGATCA	CTCGAG	TGATCACCGTTAACCATCATA

Recombinant retroviral and lentiviral packaging and cell transduction

Plasmids for retroviral packaging were co-transfected with psi-2 helper plasmid into 293T cells using the calcium chloride precipitation method. For lentiviral shRNA packaging, scrambled pLKO.1 vector or specific shRNA in pLKO.1 vector were co-transfected into 293T cells with pAX2G and pMD2G as previously described.[4] The resulting recombinant virus was collected for transduction of cells by spinoculation, followed by selection in 2 μg/mL puromycin for 3 days.

Flow cytometry analysis and cell sorting

Primary leukemic splenocytes were isolated from mice 4 or 7 days after initial corn oil or tamoxifen treatment, and AT-1 cells were harvested 6 days after 4-OHT treatment, and stained on ice in phosphate-buffered saline with 1% fetal bovine serum and analyzed on LSR II, FACS Calibur, or FACS Aria machines (BD). The antibodies used for flow cytometry are as follows: anti-mouse Gr-1 (Ly6c/Ly6g) (Cat #557979, BD or Cat #108412, BD), annexin V (Cat #550474, BD), anti-mouse CD117 (c-kit) (Cat #47-1171-80, eBioscience), anti-mouse CD11b (Cat #101228, Biolegend or Cat # 553311, BD), and anti-human CD11b (Cat #561001, BD).

The following antibodies were used for immunoprecipitation, chromatin immunoprecipitation or western blots: EZH2 (Cat#612666, BD or Cat#17-662, Millipore), C/EBPα (Cat#2295, Cell Signaling or Cat# SC-61, Santa Cruz), IgG (Abcam Cat#ab46540), Evi-1 (Cat #C50E12 Cell Signaling), menin (Cat#A300-105A, Bethyl), MLL-C (Cat#ABE240, Millipore) AF9c (Cat#A300-597A, Bethyl), H3K4m3 (Cat #ab8580, Abcam), H3K79m2 (Cat #ab3594, Abcam), H3K27m3 (Cat #17-622 Millipore), and total H3 (Cat #ab1791, Abcam).

cDNA microarray and gene set enrichment analysis

Seven control (corn oil) samples and six *Men1*-excised (tamoxifen) samples were hybridized on an Affymetrix Mouse Gene 1.0 ST chip. The data were analyzed in the statistical environment R for the quality analysis, the affyPLM library available through Bioconductor (*www.bioconductor.org*). The gene expression normalization and summarization were done using RMA from the same library mentioned above.

Principal components analysis was performed to assess similarities and differences among the samples visually. We used the Cyber-T method to identify differentially expressed genes. A multiple testing correction was applied using the p.adjust function. Gene set enrichment analysis was performed to identify gene sets that were enriched in the microarray data. Gene sets were taken from the MSigDB database.

Statistical analysis

GraphPad Prism was used for the statistical analysis. Student's t-test was used for most statistical analyses of significance, except for the Kaplan-Meier analysis, which was assessed by the log-rank test. The statistical analysis of the microarray results is detailed above.

Real-time polymerase chain reaction oligos

Mouse:

Hoxa9	F: 5'-CCACGCTTGACACTCACACT-3' R: 5'-CAGCGTCTGGTGTTTTGTGT-3'
Meis1	F: 5'-AAGGTGATGGCTTGGACAAC-3' R: 5'-TGTGCCAACTGCTTTTTCTG-3'
Gcsfr	F: 5'-CCCACCAGCTTCATCCTAAA-3' R: 5'ACTCGCTGGACCCTAGCATA-3'
Mcsfr	F: 5'-AACACTGGGACCTACCGTTG-3' R: 5'ACCGTTTTGCGTAAGACCTG-3'
Pparg	F: 5'-CAATGCACTGGAATTAGATGAC-3' R: 5'-TCTGGGTGATTCAGCTTGAG-3'
Id2	F: 5'-CTGGACTCGCATCCCACTAT-3' R: 5'-CTCCTGGTGAAATGGCTGAT-3'
Ezh1	F: 5'-TGGAAAGCAAGACGACAGCA-3' R: 5'-CGTCAGGGACACCATTCTCA-3'
Cdkn2a	F: 5'-GTACCCCGATTCAGGTGATGA-3' R: 5'-CAGTTCGAATCTGCACCGTAGT-3'
Mecom	F: 5'-GGAGGAGGACTTGCAACAAA-3' R: 5'-GACAGCATGTGCTTCTCCAA-3'
Ezh2	F: 5'-GGGACTGAAACTGGGGGAGA-3' R: 5'-CATGGAGGCTTCAGCACCAC-3'

Human:

EZH2	F: 5'-CGATGATGATGATGGAGACG-3' R: 5'-GCTGTGCCCTTATCTGGAAA-3'
HOXA9	F: 5'-CACGCTTGACACTCACACT-3' R: 5'-CGCTCTCATTCTCAGCATTG-3'
MCSFR	F: 5'-GGACATTCATCAACGGCTCT-3' R: 5'-GCTCAGGACCTCAGGGTATG-3'
PPARG	F: 5'-TGCTTGTGAAGGATGCAAGG-3' R: 5'-GAGACATCCCCACTGCAAGG-3'
ID2	F: 5'-GCAGCACGTCATCGACTACA-3' R: 5'-CACAGTGCTTTGCTGTCATTTGAC-3'
MEN1	F: 5'-CGCAAAGGCCTCTGAACTAC-3' R: 5'-GGAGAAAATCGTGGGTTTGA-3'

ChIP Oligos

Mecom	F: 5'-GTACCACCCACATTTCTTTCTCTC-3' R: 5'-CCAAAATGAATTAGTCACCACCTC-3'
Ezh2-1	F: 5'-TCCTGGAAATCCCTATGTGG-3' R: 5'-TAGATCCTGGCTGCTGACCT-3'
Ezh2-2	F: 5'-TCGCCTTTTCTTCCGTCGTC-3' R: 5'-CACTTTTGTTGGCGCCACTG-3'
Mcsfr	F: 5'-TTACCAGTTGGTCCCAGAGG-3' R: 5'-AGCAGCAACTGGAAGTCTCC-3'
Pparg	F: 5'-AGGGACAGAGTGAGGGGTCT-3' R: 5'-TTCCTGTCAGGGTCTGGAAC-3'
Id2	F: 5'-CTCCCACCCTACAGGCATT-3' R: 5'-GCGTCTTTTATGTGCACTCG-3'

References

1. Chen YX, Yan J, Keeshan K, Tubbs AT, Wang H, Silva A, et al. The tumor suppressor menin regulates hematopoiesis and myeloid transformation by influencing Hox gene expression. Proc Natl Acad Sci USA. 2006;103(4):1018-23.
2. Krivtsov AV, Twomey D, Feng Z, Stubbs MC, Wang Y, Faber J, et al. Transformation from committed progenitor to leukaemia stem cell initiated by MLL-AF9. Nature. 2006;442(7104):818-22.
3. Keeshan K, He Y, Wouters BJ, Shestova O, Xu L, Sai H, et al. Tribbles homolog 2 inactivates C/EBPalpha and causes acute myelogenous leukemia. Cancer Cell. 2006;10(5):401-11.
4. Thiel AT, Blessington P, Zou T, Feather D, Wu X, Yan J, et al. MLL-AF9-induced leukemogenesis requires coexpression of the wild-type Mll allele. Cancer Cell. 2010;17(2):148-59.

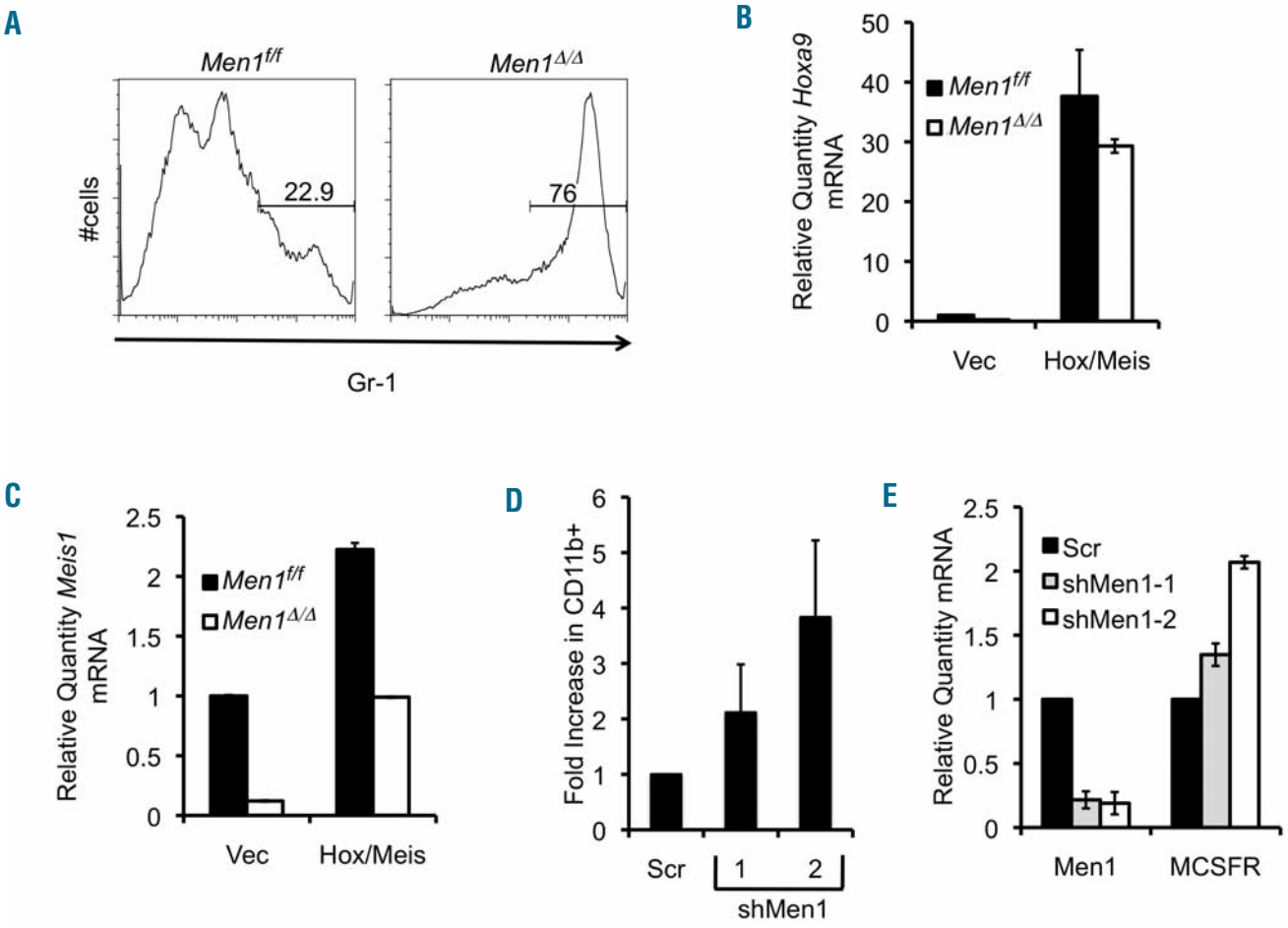

Online Supplementary Figure S1. Acute menin depletion causes MA9 cell differentiation in culture. (A) Gating for the Gr-1^{high} population in AT-1 cells 6 days after 4-OHT treatment. (B-B) Real-time PCR analysis of *Hoxa9* (B) and *Meis1* (C) transcript levels in control or *Men1*-excised AT-1 cells transduced with vector or overexpressing Hoxa9/Meis1. (D) Flow cytometry analysis of CD11b cell surface expression in Scr control and menin knockdown THP-1 cells. (E) Real-time PCR analysis of *MCSFR* transcript levels in control and menin knockdown THP-1 cells.

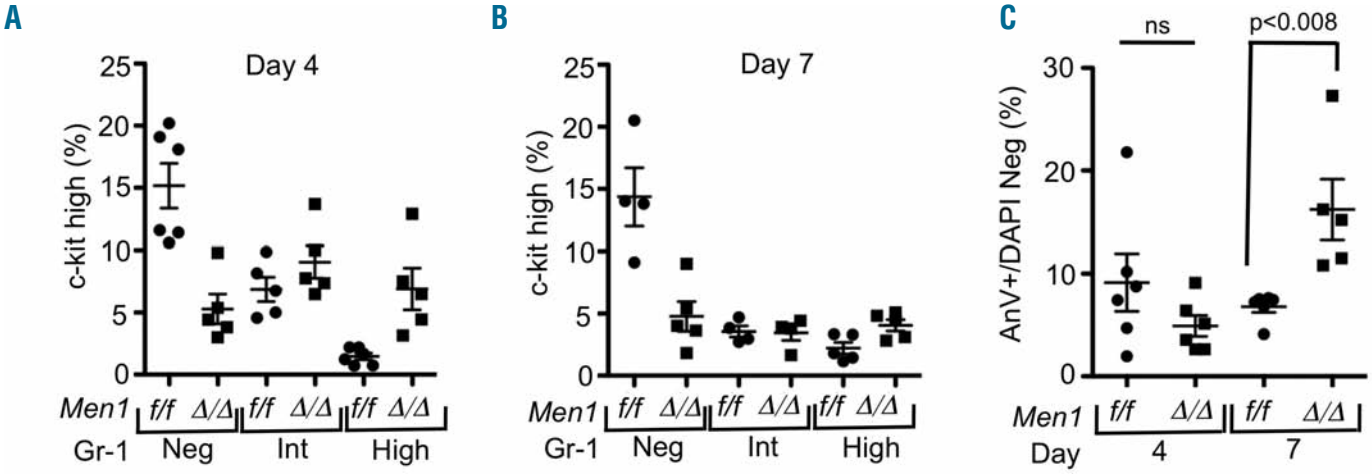

Online Supplementary Figure S2. Menin depletion causes MA9 cell differentiation *in vivo*. (A-B) Flow cytometry analysis of control and *Men1*-excised MA9 primary cells, examining c-kit^{high} cells in different Gr-1 populations. (C) Flow cytometry analysis of control and *Men1*-excised MA9 primary cells for annexin V and DAPI staining.

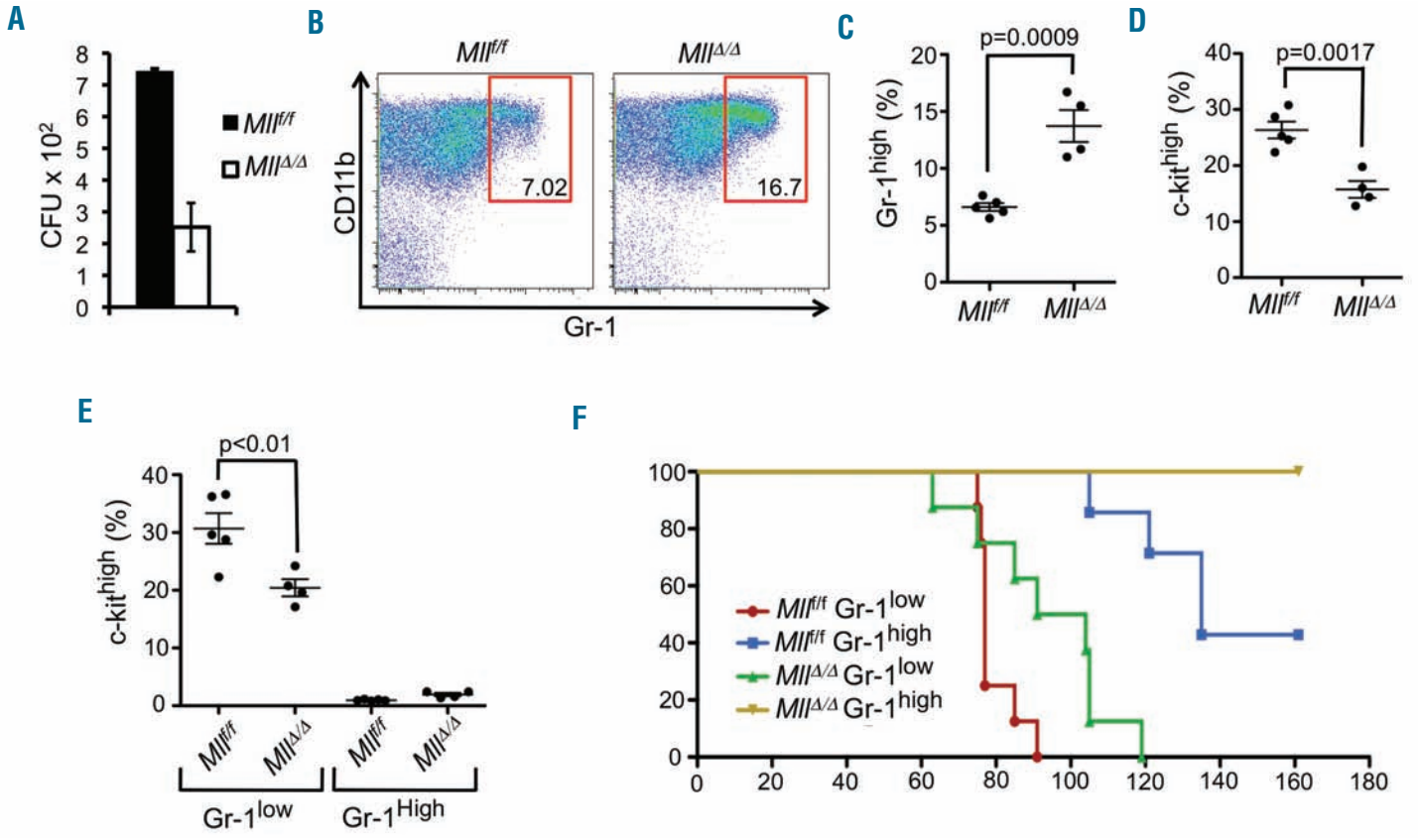

Online Supplementary Figure S3. WT MLL depletion causes MA9 cell differentiation *in vivo*. (A) Methylcellulose plating of GFP⁺ MA9 cells treated with corn oil or tamoxifen (TAM) *in vivo* 7 days after-initial treatment. (B) FACS plot for CD11b/Gr-1 in control or WT MLL-depleted MA9 cells *in vivo* 7 days after-initial TAM treatment. (C-D) A summary of flow cytometry for Gr-1^{high} (C) or c-kit^{high} (D) in control or WT MLL-depleted MA9 cells 7 days after-initial TAM treatment. (E) Analysis of c-kit^{high} cells in different Gr-1 populations in control or WT MLL-depleted MA9 cells *in vivo* 7 days after-initial TAM treatment. (F) Kaplan-Meier analysis of Gr-1^{low} and Gr-1^{high} secondary recipient mice with or without WT MLL.

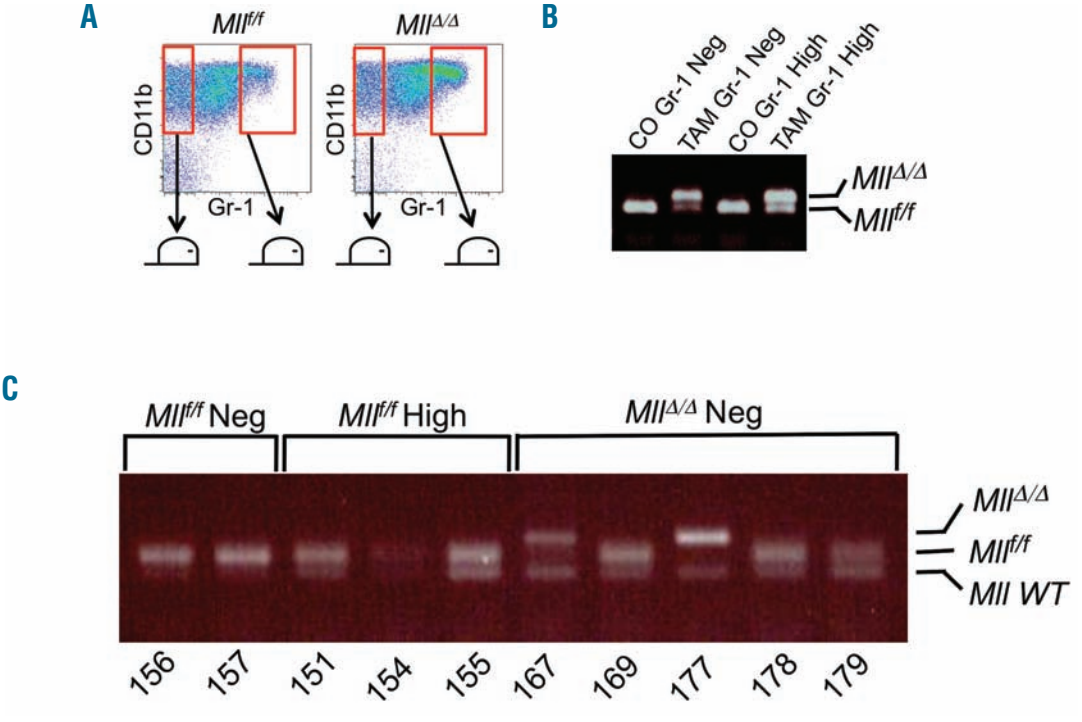

Online Supplementary Figure S4. WT MLL depletion causes MA9 cell differentiation *in vivo*. (A) A schematic for Gr-1 sorting and transplantation of MA9 cells into lethally irradiated secondary recipients. (B) Genotyping for *Mll* excision in Gr-1 sorted donor cells. (C) Genotyping of splenocytes from sacrificed secondary recipient mice for *Mll* excision.

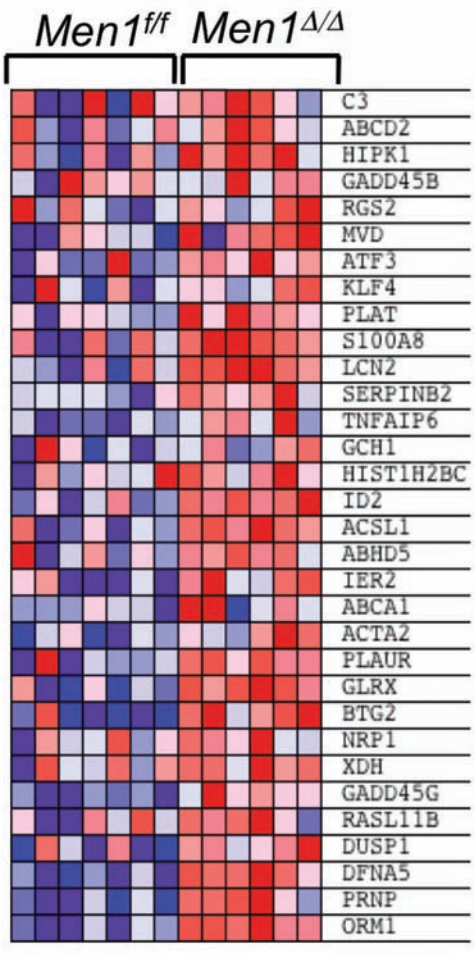

Online Supplementary Figure S5. Menin depletion causes C/EBPα target gene upregulation in MA9 leukemia cells. List of C/EBPα target genes significantly upregulated due to *Men1* excision in *Men1*$^{f/f}$; *Cre-ER* MA9 primary cells.

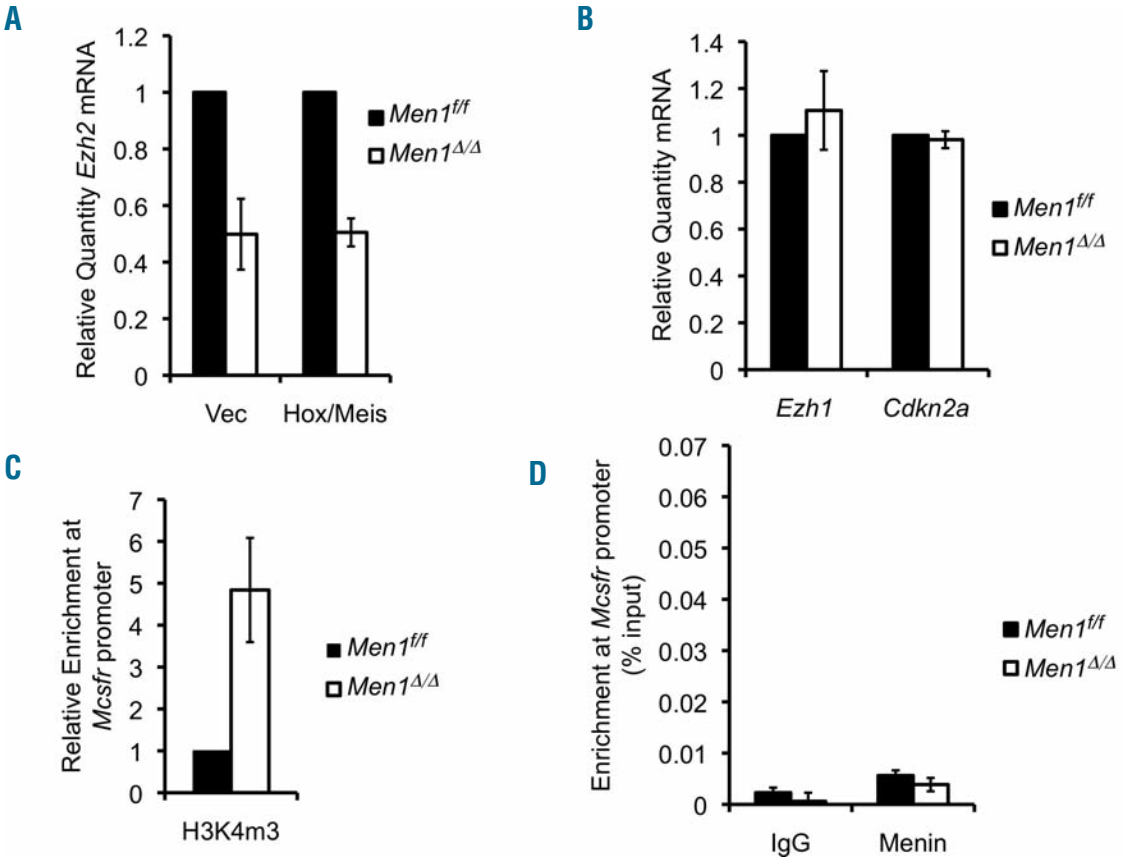

Online Supplementary Figure S6. Menin promotes EZH2 expression in MA9 cells. (A) Real-time PCR examining *Ezh2* transcript levels in control and *Men1*-excised AT-1 cells transduced with vector or overexpressing Hoxa9/Meis1. (B) Real-time PCR for *Ezh1* and *Cdkn2a* transcript levels in control and *Men1*-excised AT-1 cells. (C-D) ChIP assay for H3K4m3 (C) and menin (D) at the *Mcsfr* promoter in control and *Men1*-excised AT-1 cells.

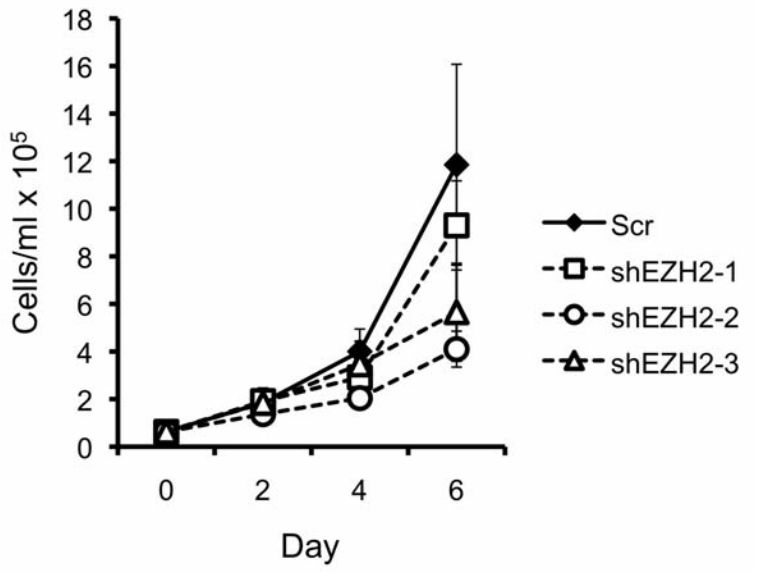

Online Supplementary Figure S7. EZH2 knockdown decreases THP-1 cell growth. Growth curve for Scr control and EZH2 knockdown THP-1 cells.